

# Strain and temperature sensitivity of a single-mode polymer optical fiber

Manuel Silva-López, Amanda Fender, William N. MacPherson, James S. Barton, and Julian D. C. Jones

*Applied Optics and Photonics Group, School of Engineering and Physical Sciences, Heriot-Watt University, Edinburgh EH14 4AS, UK*

Donghui Zhao, Helen Dobb, David J. Webb, Lin Zhang, and Ian Bennion

*Photonics Research Group, Electronic Engineering and Computer Science Division, Aston University, Birmingham B4 7ET, UK*

Received June 21, 2005; revised manuscript received August 5, 2005; accepted August 7, 2005

We have measured the optical phase sensitivity of fiber based on poly(methyl methacrylate) under near-single-mode conditions at 632.8 nm wavelength. The elongation sensitivity is  $131 \pm 3 \times 10^5 \text{ rad m}^{-1}$  and the temperature sensitivity is  $-212 \pm 26 \text{ rad m}^{-1} \text{ K}^{-1}$ . These values are somewhat larger than those for silica fiber and are consistent with the values expected on the basis of the bulk polymer properties. © 2005 Optical Society of America

OCIS codes: 060.2300, 060.2370, 120.3180, 120.6810.

Fiber optic strain sensors offer advantages that include insensitivity to electromagnetic fields, light weight, and minimal intrusiveness<sup>1</sup> compared with conventional strain gauges. Fused silica, the material of choice for the majority of optical fibers, has near-ideal mechanical characteristics for many strain-sensing applications. However, fused-silica fibers have an upper strain limit of approximately 3–5% and in general are reliable only to ~1% strain after selection of fibers by proof testing.<sup>2</sup> In highly loaded engineering structures such as highway bridges, buildings, and aircraft wings, transverse loading can result in large bending strains, which can induce locally high strains, so monitoring structural strain is becoming increasingly important. With the advent of new engineering materials, such as composites, the acceptable range of applied strain can exceed the breaking strain of fused-silica fiber, precluding the use of standard fiber-based strain gauges. The inherent fracture toughness and flexibility of polymer optical fibers (POFs) makes them much more suitable in high-strain applications than their glass-based counterparts. In addition, fiber Bragg gratings have recently been written into POFs, broadening their potential applications.<sup>3</sup>

POF sensors for strain and curvature measurement have been reported in the literature.<sup>4</sup> However, these measurements have generally been intensimetric measurements made with multimode fibers. Whereas robust sensors have been demonstrated to use intensity modulating mechanisms, they are susceptible to unwanted intensity losses, for example, bend loss or connector loss, and to variations in source power. These losses may be addressed technically, by use of additional reference power measurements, for example, but an alternative to intensity measurement is desirable. Interferometry offers a potential alternative, in which the sensing element is a length of fiber between a pair of partially reflecting splices<sup>5</sup> or a pair of matched Bragg gratings.<sup>6</sup> To produce these designs, single-mode fiber rather than

conventional multimode POF is required. The advent of single-mode POF offers the potential for high-strain fiber sensors to exploit the advantages of interferometry. We report here interferometric measurement of the optical phase sensitivities of single-mode POF versus strain and temperature changes.

The POF (Paradigm Optics) used in these experiments had a cladding diameter of  $\sim 125 \mu\text{m}$  (commercial acrylic with  $n=1.4905$ ) and a core diameter of  $6 \mu\text{m}$  [poly(methyl methacrylate) (PMMA) doped with <3% polystyrene with  $n=1.4923$ ]. It is designed to be single mode at the operating wavelength of 800 nm with an estimated cutoff wavelength of 750 nm; however, in our experiments at 632.8 nm, only the fundamental mode was observed. In all our experiments the scattering loss in the cladding and application of thermal oil or epoxy were sufficient to attenuate any cladding modes; thus only the fundamental core mode contributed to the measurement.

To study the optical properties of POF under strain, we set up a Mach-Zehnder interferometer as shown in Fig. 1. Light from a stabilized He-Ne laser (632.8 nm) was divided by a beam splitter. One beam was coupled into the fiber core, and the other trav-

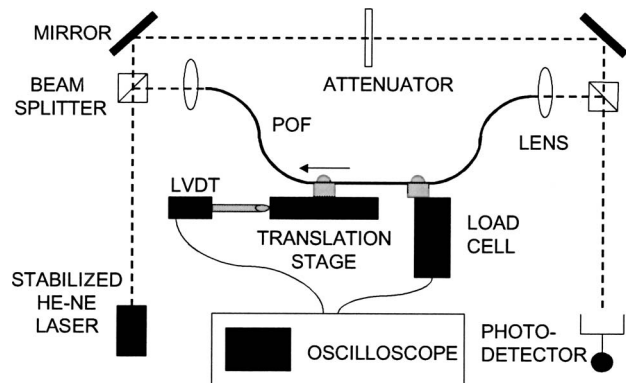


Fig. 1. Mach-Zehnder interferometer configured for fiber strain-sensitivity measurement. LVDT, displacement transducer. The source is a 632.8 nm helium-neon stabilized laser.

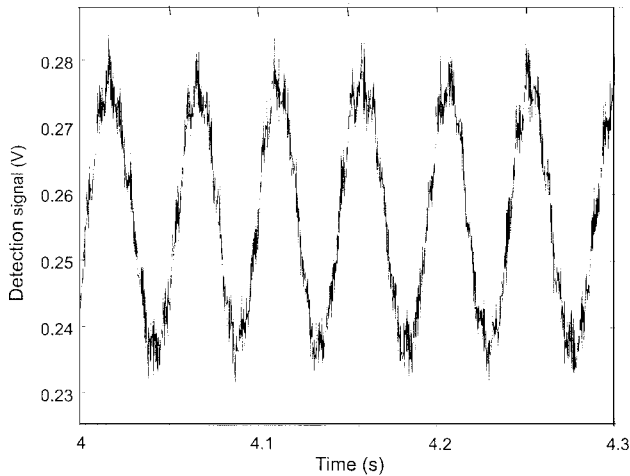


Fig. 2. Typical interference fringes during a strain cycle.

eled through free space, attenuated to optimize the fringe visibility. These beams were recombined by a second beam splitter, and the resultant interference was measured with a photodetector and an amplifier and recorded via an oscilloscope with GPIB interface to a PC for further processing.

A point on the fiber sample to be strained was attached by epoxy to a translation stage of  $\sim 10$  nm resolution. A precision displacement sensor ( $\sim 1$   $\mu$ m resolution) was used to measure the movement independently. A second point on the fiber, 108 mm from the first, was attached to a load cell. In this manner it was possible to measure the phase shift (by counting the number of fringes produced) per unit displacement caused by stretching the 108 mm section of fiber by applying a known force. Typical interference fringes are shown in Fig. 2. To optimize coupling to the fiber, we glued the ends of the POF inside silica capillaries and polished the end faces.

From the measurements of the displacement and the applied force we inferred Young's modulus to be  $2.8 \pm 0.2$  GPa, as the gradient of the linear fit to (applied stress  $\times$  length) versus displacement (Fig. 3). The phase change per unit length elongation of the fiber was derived from the slope of the data shown in Fig. 4. The average value obtained was  $131 \pm 3 \times 10^5$  rad  $m^{-1}$  at  $\lambda = 632.8$  nm.

A direct comparison with theory is complicated by the fiber drawing process, which may result in molecular alignment and consequent severe anisotropy in the material parameters of the polymer. As an illustration of the possible magnitude of this effect, we calculated the material response by using parameters appropriate to cast (isotropic) PMMA. Using a first-order theory of elasticity and the photoelastic effect, and assuming that the fiber is elastic and mechanically homogeneous, we found phase change  $d\Phi$  induced by elongation  $dL$  to be<sup>7</sup>

$$\frac{d\Phi}{dL} = \frac{2\pi n}{\lambda} \left\{ 1 - \frac{n^2}{2} [p_{12} - \nu(p_{11} + p_{12})] \right\}, \quad (1)$$

where  $\lambda$  is the wavelength,  $n$  is the refractive index,

$p_{ij}$  are Pockels coefficients, and  $\nu$  is the Poisson ratio of the fiber.

For the PMMA the Pockels coefficients are<sup>8</sup>  $p_{11} = 0.300$  and  $p_{12} = 0.297$  and the Poisson ratio is<sup>9</sup>  $\nu = 0.34$ , which gives a value  $d\Phi/dL = 132.6 \times 10^5$  rad  $m^{-1}$ , in good agreement with the experimental result. Table 1 lists the phase response  $d\Phi/dL$  of standard silica fiber,<sup>10,11</sup> that of the polymer fiber studied in this Letter, and the values predicted from theory using the coefficients for bulk PMMA.<sup>12,13</sup> The measured strain sensitivity of polymer fiber is  $\sim 14\%$  larger than that for silica fiber. In contrast, the POF Young's modulus is only  $\sim 5\%$  of that for silica fiber, reflecting the high elasticity of the polymer.

To determine the thermo-optic properties of the POF, we used the same interferometer configuration. In this case part of a second fiber sample (typically  $\sim 110 \pm 1$  mm in length) was enclosed in a heated block. The block was heated via a cartridge heater embedded in the block, and the temperature was monitored with an array of thermocouples. The temperature gradient across the heater block was minimized by applying thermal insulation around the block and restricting the heating rate to

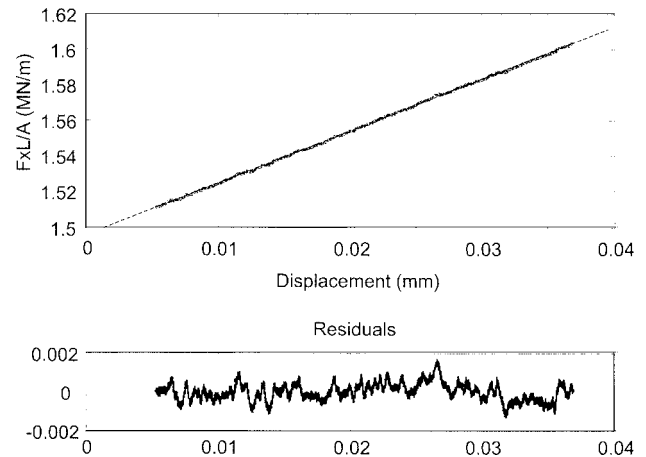


Fig. 3. Top, (applied stress  $\times$  fiber length) versus fiber extension. Young's modulus is equal to the slope of the linear fit. Bottom, residuals to the fit.

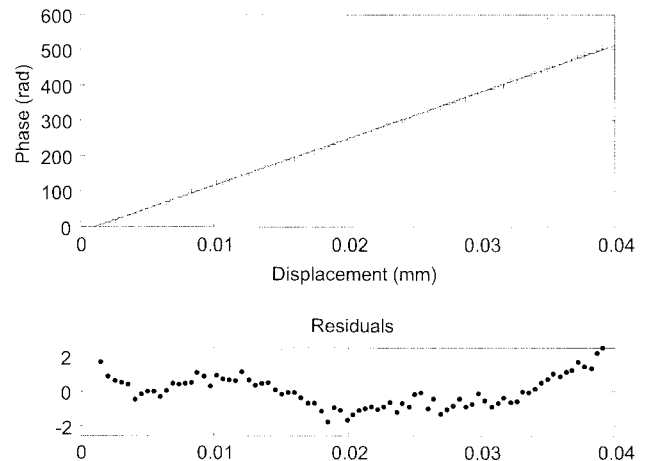


Fig. 4. Top, optical phase change versus fiber displacement. Bottom, residuals to the linear fit.

**Table 1. Comparison of Parameters of Standard Silica Fiber, Experimental Results for POF, and Values Calculated from Published Data for 632.8 nm Wavelength**

Parameter	POF	Predicted from Bulk PMMA <sup>a</sup>	Silica fiber <sup>b</sup>
$\frac{d\Phi}{dL}$ (rad m <sup>-1</sup> )	$131 \pm 3 \times 10^5$	$132.6 \times 10^5$	$115 \times 10^5$
$\frac{1}{L} \frac{d\Phi}{dT}$ (rad m <sup>-1</sup> K <sup>-1</sup> )	$-212 \pm 26$	-154.3	99.8
Young's modulus (GPa)	$2.8 \pm 0.2$	3.3	71.70

<sup>a</sup>Refs. 12 and 13.

<sup>b</sup>Refs. 10 and 11.

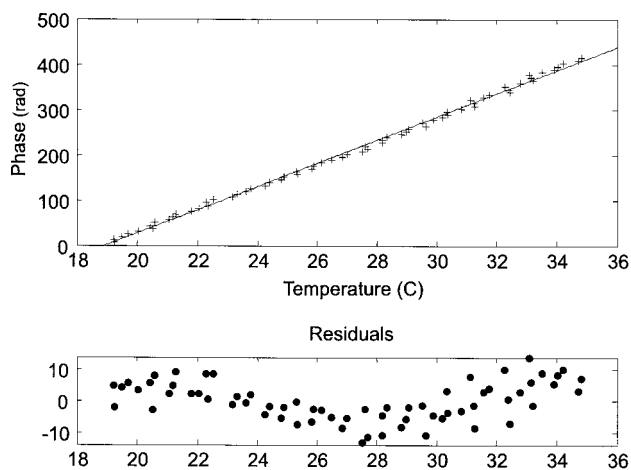


Fig. 5. Top, optical phase change versus fiber's average temperature. Bottom, linear fit.

$\sim 1$  °C min<sup>-1</sup>. A temperature gradient of less than 0.5 °C along the length of the fiber was obtained in this way. Additional thermocouple measurements verified that the fiber protruding from the edges of the heater block remained at room temperature during the experiment, and to maximize thermal transfer between the heater block and the fiber a thermal grease was applied. Following the same procedure as for the strain measurements, we determined the phase as a function of the average temperature (Fig. 5) to get a value, after normalizing for heated fiber length, of  $d\Phi/dT = -212 \pm 26$  rad m<sup>-1</sup> K<sup>-1</sup>.

A change in fiber temperature  $dT$  causes an optical phase change  $d\Phi$  that results from thermal expansion of the fiber and a change in the refractive index of the core (thermo-optic effect):

$$\frac{d\Phi}{dT} = \frac{2\pi}{\lambda} \left( n_0 \frac{dL}{dT} + L_0 \frac{dn}{dT} \right) = \frac{2\pi}{\lambda} L_0 (n_0 \alpha + \beta). \quad (2)$$

For PMMA, the coefficient of thermal expansion,  $\alpha$ ,

and thermo-optic coefficient  $\beta$  are,<sup>7,11</sup> for our temperature range,  $\alpha = 70 \times 10^{-6}$  K<sup>-1</sup> and  $\beta = -1.2 \times 10^{-4}$  K<sup>-1</sup> and, taking  $n_0 = 1.4923$  and  $\lambda = 632.8$  nm, we calculated the temperature sensitivity per unit length, using Eq. (2), to be  $-154.3$  rad m<sup>-1</sup> K<sup>-1</sup>, or 73% of the measured value. Again, a comparison of experimental and theoretical PMMA values is given in Table 1. It is interesting to note that, in contrast to silica, the polymers have a negative thermo-optic coefficient, owing to the predominant effect of the density change with temperature. The maximum operating temperatures (typically 80 °C to 120 °C) of polymer fibers are sufficient for many structural-characterization experiments.

The strain and temperature sensitivities of a PMMA polymer optical fiber have been measured experimentally at 632.8 nm and calculated from published values for bulk PMMA. The temperature sensitivity may be subject to effects from core doping and fiber drawing. In both quantities there is a general consistency between the measured fiber properties and the estimates from bulk PMMA. Both strain and temperature sensitivities of the polymer fiber were somewhat larger than those for silica fiber. Coupled with the high yield strain of polymers, this higher sensitivity is potentially advantageous in the field of interferometric fiber optic sensing.

We thank the UK Engineering and Physical Sciences Research Council (EPSRC) and the UK Defence Science and Technology Laboratory for funding through the Joint Grant Scheme, and W. N. MacPherson acknowledges Advanced Fellowship Programme funding from the EPSRC. J. S. Barton's email address is j.s.barton@hw.ac.uk.

## References

1. J. M. López-Higuera, ed., *Handbook of Optical Fiber Sensing Technology* (Wiley, 2002).
2. M. Komachiya, R. Minamitani, T. Fumino, T. Sakaguchi, and S. Watanabe, *Appl. Opt.* **38**, 2767 (1999).
3. H. Y. Liu, H. B. Liu, G. D. Peng, and P. L. Chu, *Opt. Commun.* **220**, 337 (2003).
4. K. S. C. Kuang, W. J. Cantwell, and P. J. Scully, *Meas. Sci. Technol.* **13**, 1523 (2002).
5. C. E. Lee, J. J. Alcoz, Y. Yeh, W. N. Gibler, R. A. Atkins, and H. F. Taylor, *Smart Mater. Struct.* **1**, 123 (1992).
6. M. G. Shlyagin, P. L. Swart, S. V. Miridonov, A. A. Chtcherbakov, I. M. Borbon, and V. V. Spirin, *Opt. Eng.* **41**, 1809 (2002).
7. C. D. Butter and G. B. Hocker, *Appl. Opt.* **17**, 2867 (1978).
8. R. M. Waxler, D. Horowitz, and A. Feldman, *Appl. Opt.* **18**, 101 (1979).
9. D. D. Raftopoulos, D. Karapanos, and P. S. Theocaris, *J. Phys. D* **9**, 869 (1976).
10. A. Bertholds and R. Dandliker, *J. Lightwave Technol.* **6**, 17 (1988).
11. B. J. White, J. P. Davis, L. C. Bobb, H. D. Krumboltz, and D. C. Larson, *J. Lightwave Technol.* **5**, 1169 (1987).
12. J. M. Cariou, J. Dugas, L. Martin, and P. Michel, *Appl. Opt.* **25**, 334 (1986).
13. J. Brandrup, E. H. Immergut, and E. A. Grulke, eds., *Polymer Handbook* (Wiley, 1999).